

Gravitational Drainage of Compressible Organic Materials

Morten Lykkegaard Christensen, Dominik Marek Dominiak, Per Halkjær Nielsen,
and Kristian Keiding

Dept. of Biotechnology, Chemistry and Environmental Engineering, Aalborg University,
Sohngaardsholmvej 49 and 57, 9000 Aalborg, Denmark

Maria Sedin

Dept. of Chemical and Biological Engineering, Chalmers University of Technology, Göteborg, Sweden

DOI 10.1002/aic.12222

Published online May 12, 2010 in Wiley Online Library (wileyonlinelibrary.com).

A model was developed to simulate drainage of compressible particle suspensions, and study how cake compression and volumetric load influence the process. The input parameters were settling velocity, cake resistance and compressibility. These parameters were found using a new experimental method. Dextran-MnO₂ particle suspensions were drained as these resemble organic waste slurries with respect to settling and compressibility. It was demonstrated that cake compressibility must be taken into account to obtain adequate simulations. This implies that pressurized filtration resistances cannot be used for drainage simulations. In the filtration step, a distinct increase of dry matter from top to bottom of the cake was observed. During the subsequent consolidation, the cake compressed and a uniform dry matter profile was found. The final dry matter content of the cake increased with feed concentration and volumetric load. The drainage time increased proportionally with feed concentration and, more importantly, proportionally with squared volumetric load. © 2010 American Institute of Chemical Engineers AICHE J, 56: 3099–3108, 2010

Keywords: dewatering, settling, manure, sludge, specific cake resistance

Introduction

Organic waste products such as biological sludge and animal manure can be used for heat and power generation, used as fertilizer in agricultural systems, or converted to transportation biofuels.^{1,2} Furthermore, it is possible to convert organic waste into substances that can be used in various industrial products.² As the concentration of dry material is low in sludge and manure, solid-liquid separation is an important part of pretreatment in order to lower transportation costs, minimize the need for storage capacity, or increase the energy output from incineration. There are several methods for solid-liquid separation, including gravity drainage; for

example, organic slurries can be drained using belt filter presses³ or sludge drying reed beds.⁴ The critical pressure above which the dewatering rate is constant has been determined to be in the range of 5–50 kPa for biological sludge.⁵ Operation at pressures above the critical pressure have only a limited effect on separation performance, because cake porosity decreases and hydraulic resistance, therefore, increases with pressure. Gravity drainage, is, thus, an energy-efficient means of dewatering organic waste products as the pressure is close to the critical pressure, so little energy is wasted on cake compression.

In designing and optimizing gravity drainage processes, a mathematical model and laboratory-scale measurements of settling velocities, cake compressibility and cake resistance would be helpful. In the case of cake resistance, most methods described in the literature measure the resistance at pressures higher than 100 kPa.⁶ These pressures are higher than

Correspondence concerning this article should be addressed to M. L. Christensen at mlc@bio.aau.dk.

the critical pressure of organic materials and higher than the pressures usually observed during gravity drainage. Applying such high pressures leads to the problem of transforming and applying the obtained cake resistances to the low-pressure conditions encountered in gravity drainage experiments. Furthermore, studies that describe the gravity drainage processes of inorganic particles^{7,8} and biological sludge,^{3,9} for example, do not include cake compression in the model. Cake compression may influence the drainage processes, but it is not known whether cakes are compressible at the low pressure achieved during drainage. However, most organic cakes are highly compressible at high pressure (>100 kPa), so it might be expected that organic cakes are compressible at lower pressures as well. In that case, existing drainage models must be modified before application to organic slurries.

The settling velocity is usually determined from sedimentation experiments and decreases with particle concentration.¹⁰ However, it is not known whether the settling velocity changes with drainage rate or to what extent settling influences the drainage process. Thus, to predict how, for example, feed concentration, load, and media resistance influence the drainage process, it is necessary to know whether or not settling is important for the drainage process and, if so, how the settling velocity can be determined.

Several experiments are required to find out how cake resistance, cake compressibility and settling influence the gravity drainage of organic slurries. However, organic slurries are often complex mixtures, so it is difficult to use organic slurries for such studies. Alternatively, simpler model compounds can be used; for example, dextran-MnO₂ particles have been used in pressure filtration studies.¹¹ The compressibility of dextran-MnO₂ particles is comparable to that of other organic materials, such as biological sludge.¹¹ Moreover, it is easy to measure the porosity profile through dextran-MnO₂ cakes due to the higher γ -ray attenuation of MnO₂ than of water or ethanol. For that reason, dextran-MnO₂ particles are a good candidate for studying separation processes in organic compounds.

This study aims (1) to develop an experimental method for measuring settling velocity, cake resistance and cake compressibility, (2) to clarify how media resistance, cake compression and settling influence the drainage process, and (3) to simulate the drainage process to determine how load influence the final dry matter content of the drained cake. Dextran-MnO₂ particles will be synthesized and drained; local cake porosity will be monitored online at high-spatial resolution to investigate cake inhomogeneity and cake compression during the experiments.

Experimental

Dextran-MnO₂ particles

Dextran-MnO₂ particles were synthesized according to Hwang et al.¹¹ Before particle production, 0, 1, 2, and 3 g of 400–500 kDa *Leuconostoc mesenteroides* dextran (Sigma-Aldrich, St. Louis, MO) were suspended in 100 mL of 99.9% v/v ethanol. Particles were then prepared by adding 100 mL of the dextran suspension to 100 mL of 1.5% w/w KMnO₄ solution. The dextran suspension was added gradually (5 mL of dextran suspension per addition), and after

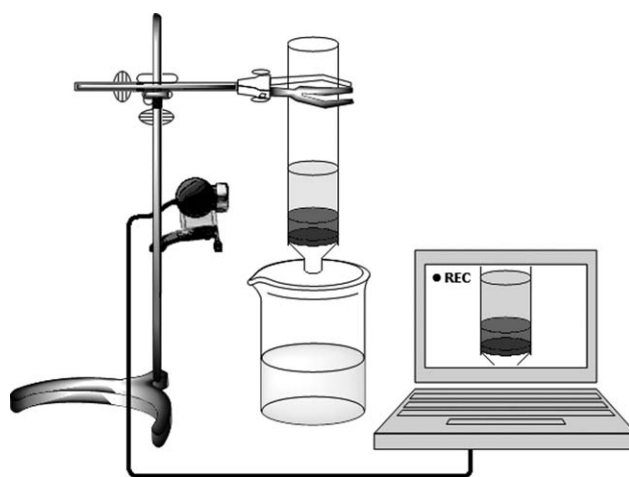


Figure 1. Sketch of drainage equipment used.

each addition, the mixture was stirred at 600 rpm for 20 s and then at 400 rpm for 40 s. An overhead stirrer (RZR 2041; Heidolph Instruments, Schwabach, Germany), and an impeller (BR 13; Heidolph) were used. After preparing the dextran-MnO₂ particles, the suspension was analyzed using a LSM510 confocal scanning laser microscope (CLSM; Carl Zeiss, Oberkochen, Germany) at 10 \times magnification. Large dextran-MnO₂ particles (up to 500 μ m) were formed, but the suspension also contained nonfloculated MnO₂ particles (1–10 μ m). The produced particles settled overnight at room-temperature and supernatant was withdrawn until the desired concentration was achieved (8–45 g/L). The suspension was then gently mixed and used in the dewatering experiments.

Gravity drainage and sedimentation

A series of gravity drainage experiments was performed. During drainage, a cake was formed on the filter media. It was observed that the particles settled during drainage. For that reason, a sedimentation experiment was setup, as well as to compare the settling velocity determined during the gravity drainage and sedimentation experiments.

Samples of 100 or 200 mL were drained using a 40-cm-high-transparent glass cylinder fitted with a Whatman no. 41, 20–22 μ m cut-off, filter article (Whatman, Maidstone, U.K.) placed at the bottom of the cylinder (Figure 1). The internal diameter of the cylinder was 6 cm, more than 1,000 times larger than the dextran-MnO₂ particles. If the dextran-MnO₂ particles behaved like individual particles, the reduction in settling velocity due to wall effects would then be less than 5%.¹² A digital camera was placed roughly 10 cm away from the cylinder and used to monitor the drainage process. The images were analyzed to determine the distance between (1) the filter media and the interface between the suspension and the clear liquid phase ($height_I$), as well as (2) the filter media and the interface between the clear liquid and the surrounding air ($height_{II}$). Sedimentation experiments were performed using the same setup, but with an impermeable media at the bottom of the glass cylinder. Hence, datasets of time, $height_I$, and $height_{II}$ were obtained.

The local solid-mass fraction was measured at different positions in the cake using a ²⁴¹Am source that emits γ -rays

at 59.54 keV. The attenuation was measured using an NaI(Tl) scintillation detector and integrating the number of counts between 58 and 83 keV. The calibration curve was acquired by measuring the attenuation of the feed suspension, as well as the attenuation of the final cake, the solid-mass fraction of which was known.¹³ It was found that $\mu_{\gamma, \text{filtrate}} = 17.7 \text{ m}^{-1}$ and $\mu_{\gamma, \text{particles}} = 56.0 \text{ m}^{-1}$.

The filtrate viscosity was measured to be $2.4 \times 10^{-3} \text{ Pa s}$ using a KPG no. 100 capillary viscometer (Cannon-Fenske, State College, PA), and the filtrate density was measured to be 940 g/L by weighting the filtrate volume during the experiments. The measured values were similar to the viscosity and density of 50% v/v ethanol. The resistance of the media was found by filtering 200 mL of 50% v/v ethanol through a clean Whatman no. 41 filter paper and was calculated to be $9.7 \times 10^7 \text{ m}^{-1}$. After one of the experiments, 50% v/v ethanol was filtered through the used filter paper, and no increase in R_{mem} was observed afterwards. The cakes were easily removed from the filter media.

Analysis of cake

The dry matter content of the cake was measured by weight loss after drying at 104°C overnight. The amount of organic material was determined by measuring the loss on ignition after 4 h at 500°C. The determined ratio between organic and inorganic materials nicely fit the ratio between added dextran and MnO_2 , assuming that all KMnO_4 was reduced to MnO_2 (slope 0.99 ± 0.06 , intercept 0.0 ± 0.1). The suspension changed color from purple to brown when dextran was added to KMnO_4 , which confirmed the reduction of MnO_4^- to MnO_2 .

The solid-volume fraction of the filter cake was calculated from the measured dry matter content, as follows

$$\phi = \frac{\varphi}{\varphi + (1 - \varphi) \frac{\rho_s}{\rho_L}} \quad (1)$$

The particle density was measured by producing 25 g of the particles. The particles were filtered and dried overnight at 104°C. The dried cake was crushed and dissolved in 200 mL of demineralized water in a 500-mL pycnometer. Air bubbles were removed by placing the pycnometer *in vacuo* for 1 h. The pycnometer was then filled with degassed demineralized water and weighted. After that, the dry content of the sample was found by drying the sample at 104°C overnight. The density of dextran- MnO_2 particles ($\text{dextran}/\text{MnO}_2 = 2.7 \text{ g/g}$) was determined to be $1950 \pm 10 \text{ g/L}$.

Theory of the Drainage Process

The drainage process can be simulated if average specific cake resistance, cake compressibility, and settling velocity are known. To do this, the drainage rate v_d , must be calculated, which can be done using Eq. 2³

$$v_d = \frac{\Delta P}{\eta(\alpha_{\text{cake}} \omega + R_m)} \quad (2)$$

where the pressure difference is given as

$$\Delta P = \frac{Mg}{A} = \rho g h_t + c g h_0 \left(1 - \frac{\rho}{\rho_s}\right) - \omega g \quad (3)$$

As can be seen in Eq. 2, the drainage rate is directly related to the average specific cake resistance. Furthermore, the drainage rate is indirectly related to cake compressibility and settling velocity. Cake compressibility describes how the solid-volume fraction of the cake changes with pressure; the compressibility influences the drainage rate indirectly because the average specific cake resistance increases with solid-volume fraction. Settling is important because the cake grows faster if the settling velocity is high. This affects the drainage process because the drainage rate decreases with cake thickness.

Average specific cake resistance, settling velocity, and cake compressibility can be determined from the introduced laboratory experiments discussed here. To estimate the three parameters, it is practical to divide the drainage process into three stages: (A) cake formation, (B) pure filtration, and (C) cake collapse (Figure 2). Settling velocity can only be determined using data obtained during cake formation (stage A). Average specific cake resistance is most easily determined using data obtained during pure filtration (stage B), and cake compressibility is most easily determined using data obtained after final cake compression (stage C). The procedure used will be described in the following sections. When all parameters are determined, the level of the sample, i.e., the drainage rate, can be simulated numerically using Eq. 2, and Euler's method as $dh/dt = v_d$. Such simulation can be used to study the impact of different input parameters on the drainage process.

Cake formation (Stage A)

During the initial part of the process when $t < t_1$, a cake builds up on the media (stage A), and the cylinder consists of cake, suspension, and clear liquid phases (Figure 2); the total level of the sample is $h_t = h_w + h_s + h_c$. Furthermore, cake height is a function of the amount of cake deposited on the media and of the dry matter content of the cake

$$h_c = \frac{\omega}{\phi \rho_s} \quad (4)$$

and

$$\omega = S(h_0 - h_t) + S v_s t \quad (5)$$

where S is given as⁶

$$S = \frac{1}{\frac{1}{\rho_s} \left(\frac{\rho_s}{c} - 1 \right) - \frac{m-1}{\rho}} \quad (6)$$

If the settling velocity is zero, ω increases proportionally with the specific filtrate volume ($h_0 - h_t$). If particles settle, the cake builds up faster and a clear liquid phase develops above the suspension. The height of clear water can be calculated using Eq. 7

$$h_w = v_s \cdot t \quad (7)$$

As h_w is measured during the drainage experiments, it is possible to calculate the settling velocity by plotting h_w as a function of time and using linear regression. The same method can be used to estimate the settling velocity from the results of the settling experiment.

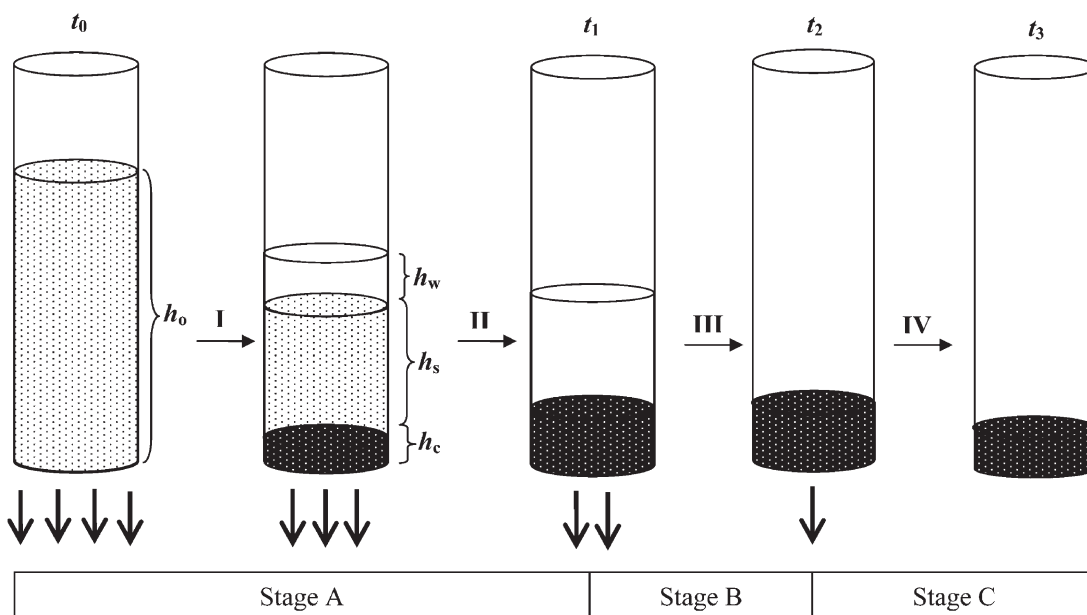


Figure 2. Principle of drainage experiment.

Pure filtration (Stage B)

All particles are deposited on the media and the liquid above the cake is filtered through the cake when $t_1 \leq t < t_2$ (Figure 2). The amount of deposited cake is constant and equals $\omega = ch_0$. It is possible to derive an equation for the sample level h_t , throughout the stage. Equation 8 has been derived assuming that $\rho h_t \gg c(1 - \rho/\rho_s)h_0 - \omega$, inserting $\omega = ch_0$ into Eq. 2 and integrating

$$h_t(t) = h_t(t_1) \cdot e^{-\chi(t-t_1)} \quad (8)$$

where

$$\chi = \frac{\rho g}{\eta(\alpha ch_0 + R_m)} \quad (9)$$

Furthermore, h_w is given as the level of the sample minus the cake height

$$h_w = h_t - h_c = h_t(t_1) \cdot e^{-\chi(t-t_1)} - \frac{ch_0}{\phi \rho_s} \quad (10)$$

It is, therefore, possible to estimate χ by fitting Eqs. 8 or 10 to experimental data. When χ is known, Eq. 9 can be used to calculate the average specific cake resistance.

Cake collapse (Stage C)

All liquid has been drained through the cake when $t \geq t_2$. Thus, air reaches the cake surface and menisci are formed between the solid particles (Figure 2). This generates a capillary pressure, and, thereby, a drag on the cake structure.¹⁴ Organic materials form highly compressible cakes, so the cake porosity is higher at the top of the cake than at the bottom. Thus, the cake will collapse because the cake cannot

withstand the drag on the cake structure.¹⁴ The compression starts at the cake surface, while the underlying cake compresses when the capillary pressure exceeds the local compressible yield stress. The compressible yield stress increases with the solid-volume fraction; hence, cake collapse and final dry matter content are derived from the relationship between the solid-volume fraction and the compressible yield stress. An often used constitutive equation for the compressible yield stress is given in Eq. 11^{15,16}

$$p_y = p_a \left(\left(\frac{\phi}{\phi_0} \right)^{1/\beta} - 1 \right) \quad (11)$$

The process stops when the liquid pressure at the sample-media interface is zero. The liquid pressure can be calculated using Eq. 12

$$p_l^{\text{mem}} = \rho g h_t + g \omega \left(1 - \frac{\rho}{\rho_s} \right) - p_s^{\text{mem}} \quad (12)$$

and is zero when

$$p_s^{\text{mem}} = \rho g h_c + \Delta \rho g h_c \phi \quad (13)$$

as $h_c = h_t$ at the end of the drainage experiment, and $\omega = h_c \phi \rho_s$ according to Eq. 4. The drag at the top of the cake, which results from the capillary forces, then equals $\rho g h_c$, and the effective pressure increases from $\rho g h_c$ at the top of the cake to $\rho g h_c + \Delta \rho g h_c \phi$ at the bottom. If $\Delta \rho \phi \ll \rho$, it can be assumed that the effective pressure and solid-volume fraction are constant throughout the thickness of the cake. The final cake height can then be obtained by combining Eqs. 11 and 13 setting $p_s^{\text{mem}} = p_y$

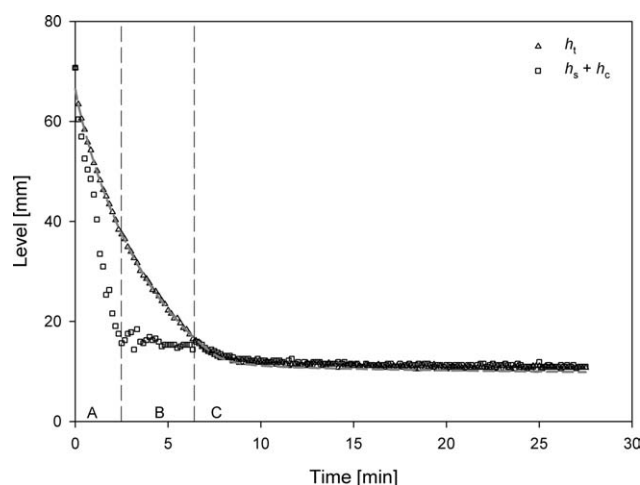


Figure 3. Drainage of a suspension of 12 g/L dextran-MnO₂ particles.

The actual level of the suspension is shown (h_t), as well as the level of the water-suspension interface ($h_c + h_s$).

$$h_{c,\infty} = \frac{p_a}{\rho g} f(\phi) \quad (14)$$

where

$$f(\phi) = \frac{(\phi/\phi_0)^{1/\beta} - 1}{1 + \phi \frac{\Delta\rho}{\rho}} \quad (15)$$

Both the cake height and the solid-volume fraction can be measured at the end of the experiment. From a series of experiments in which different amounts of solid materials are drained it is, therefore, possible to determine p_a , β , and ϕ_0 by fitting Eq. 14 to the experimental data. To lower the number of adjustable parameters ϕ_0 has been determined separately; ϕ_0 is the solid-volume fraction where particles just form a continuous network—the so-called gel point. An estimate of ϕ_0 can therefore be made from the results of settling experiments in which the effective pressure is low, i.e., $p_s^{\text{mem}} = \omega g(1 - \rho/\rho_s)$, and the solid-volume fraction of the formed cake is close to, but greater than ϕ_0 .

Results and Discussion

Description of gravity drainage setup

Figure 3 shows data from a typical gravity drainage process. Three different stages (cf. Figure 2) can be identified: stage A in which particles settle and the cake builds up, stage B in which liquid is filtered through the nongrowing cake, and stage C in which the liquid-air interface reaches the cake surface and the cake collapses. The transition between stages A and B is the time at which $h_s = 0$, i.e., when the suspension vanishes. Furthermore, the transition between stages B and C is found at the time at which $h_w = 0$, i.e., when the pure water vanishes. The pressure at the sample-media interface was calculated from the sample level, and from these calculations it was found that the pressure decreased from roughly 650 Pa at the onset of the experiment to 90 Pa at its end.

Determination of specific cake resistance and settling velocity

The data presented in Figure 3 were used to estimate the specific cake resistance and the settling velocity. This was done by measuring the height of the clear water phase, which increased during cake formation (stage A) and disappeared again during the pure filtration stage (stage B). Figure 4a shows the calculated values of h_w .

The settling velocity was determined during cake formation (stage A), and the result was compared with the settling velocity determined from a simple sedimentation experiment. For the gravity drainage experiment, the settling velocity was determined from the initial increase in h_w (Figure 4a). It was observed that h_w increased linearly until $t_1 = 2$ min and 20 s. Equation 7 was fitted to the measured data obtained during stage A (Figure 4b), and the settling velocity was calculated to be 1.6×10^{-4} m/s. Data from the sedimentation

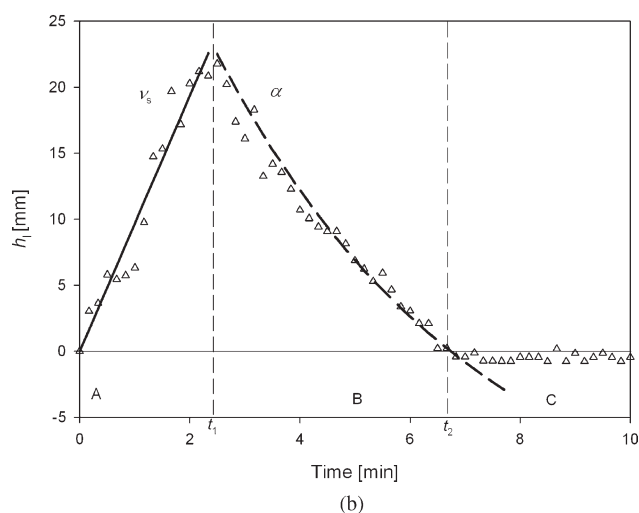
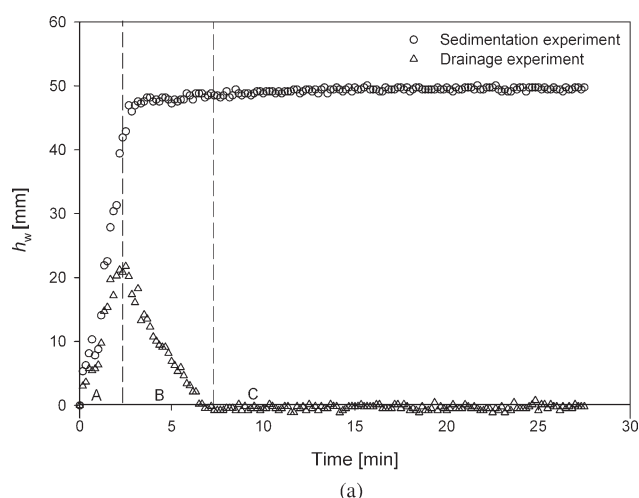


Figure 4. The height of the clear liquid phase (h_w) in the gravity drainage experiment shown in Figure 3, i.e., a suspension of 12 g/L dextran-MnO₂ particles.

(a) Data from the drainage experiment, as well as a sedimentation experiment, and (b) data from the drainage experiment and simulated data for stage A (solid line), and stage B (dotted lines).

Table 1. Experimental Data for Drainage of Dextran-MnO₂ Suspensions of Varying Feed Concentrations

Concentration [g/L]	Settling velocity [m/s]	Resistance [m/kg]	Cake height [mm]	Dry matter content
8	1.9×10^{-4}	3.2×10^9	15.5	0.084
19	1.2×10^{-4}	1.7×10^9	19.7	0.10
29	1.2×10^{-4}	1.5×10^9	31.3	0.11
45	3.1×10^{-5}	1.5×10^9	42.6	0.12

experiment are included in Figure 4a. The settling velocity was almost identical during both drainage and sedimentation. Thus, simple sedimentation experiments can be performed to determine the settling velocity relevant to drainage experiments. Settling can influence the drainage process, because settling affects cake buildup. The impact of settling on the drainage rate will be discussed in section “Simulation of Gravity Drainage Processes.”

Specific cake resistance is a parameter that describes how difficult it is to dewater a given material. Using the method presented here, it is possible to calculate the specific cake resistance obtained during gravity drainage processes and compare this value with the resistance determined during pressure filtration processes. The specific cake resistance was determined during pure filtration (stage B). The total resistance was calculated to be $1.2 \times 10^9 \text{ m}^{-1}$ by fitting Eq. 8 to the measured values of h_w obtained during stage B (Figure 4b). The total resistance was given as the sum of the cake resistance and the media resistance. Using the measured media resistance of the clean filter paper, the average specific cake resistance was calculated to be $1.2 \times 10^9 \text{ m/kg}$. This resistance was lower than the resistance obtained from piston filtration experiments (approximately $4 \times 10^{12} \text{ m/kg}$ at 1 bar).¹¹ Thus, the cake was more loosely packed after the drainage experiment than were cakes formed during piston filtration. The measured resistance indicates that it is impossible to increase the dewatering rate using higher pressure because the specific cake resistance increases almost proportionally with pressure. Drainage is, therefore, a good method for initially dewatering organic material. If high-dry matter content is needed, drainage must be combined with cake consolidation.

The settling velocity and specific cake resistance were calculated from four drainage experiments in which the feed concentration of dextran-MnO₂ particles in the sample was varied between 8 and 45 g/L (Table 1). The settling velocity decreased with particle concentration. This has often been observed and explained as a result of hindered settling, i.e., hydrodynamic interaction between particles.¹⁷ Different mathematical expressions exist for estimating the relative settling velocity from the volume fraction of the particles, i.e., $v_s(\text{relative}) = (1 - \phi_p)^{4.65}$.¹⁰ However, the particles are water swollen in this case, and if the volume fraction is calculated from the mass and the density of the *dry* materials, the relative settling velocity is underestimated. At 45 g/L, the estimated relative settling velocity has been calculated to be 0.9, whereas it has been *measured* to be <0.2. The conclusion is that the settling velocity must be determined experimentally as a function of concentration, i.e., from simple sedimentation experiments or drainage experiments.

The apparent average specific cake resistance has been estimated as well (Table 1). The resistance was highest for

the sample with the lowest particle concentration. This could be because the filter media resistance was underestimated and the average specific cake resistance, therefore, overestimated. This had a considerable impact on the calculated resistance when the formed cake was thin and the total cake resistance low. At higher particle concentrations, the resistance was constant and independent of concentration. This was reasonable because the initial height of the suspension, and, therefore, the pressure drop across the cake, was the same in all four experiments.

Cake compressibility

The dextran-MnO₂ cakes were highly compressible. This was, for example, observed from the data shown in Figure 3, where the cake collapsed during the final stage of the drainage process. During this part of the process, the dry matter content of the cake increased from 6.4% g/g to 9.0% g/g. Moreover, the dry matter content of the cake formed during the sedimentation experiment was estimated to be 4.6% g/g (i.e., $\phi_0 = 0.023$). This dry matter content was lower than that of the cake formed during drainage. Thus, the extra drag on the cake structure from the liquid flow contributed to the cake compression. The effective pressure at the bottom of the cake was calculated to be $p_s^{\text{mem}} = \omega g(1 - \rho/\rho_s) = 4 \text{ Pa}$ during sedimentation, compared with 90–650 Pa during drainage. The effective pressure at the bottom of the cake is a function of both feed concentration and load. As cake compression increases both cake porosity and specific cake resistance, both the drainage rate and the final dry matter content increases with load and feed concentration.

To study cake compressibility in more detail, the local solid-mass fractions were measured online. Figure 5 shows the local solid-mass fractions measured at four different positions in the cake, i.e., 2, 3, 5, and 7 mm from the top of the filter media. Notice that after 28 min, the cake height was lower than 7 mm, which is why no more measurements were made at this depth. The data measured 3 mm above the filter media will now be discussed. During initial cake buildup (stage A), the solid-mass fraction increased to 8% g/g; during

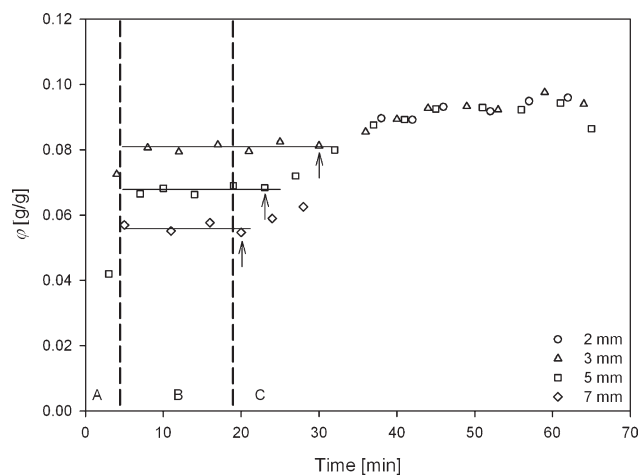


Figure 5. Local solid-mass fraction of the cake formed when draining dextran-MnO₂ particles.

The solid-mass fraction was measured online at different positions above the filter media.

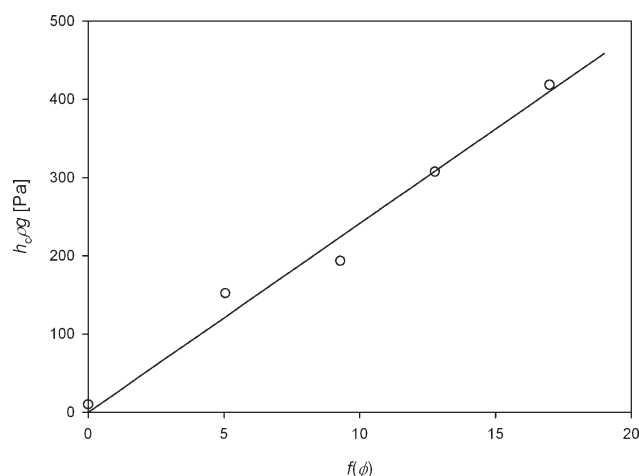


Figure 6. Cake compressibility. Data from four different drainage experiments (Table 1), and a sedimentation experiment.

The final dry matter content was measured at the end of the experiments and Eq. 15 was used to calculate $f(\phi)$. The final structural pressure was calculated and plotted as a function of $f(\phi)$.

stage B, the mass fraction was constant. The solid-mass fraction remained constant during stage C, until the solid-mass fraction of the cake exceeded 8% g/g; the solid-mass fraction then increased to 9.5% g/g. Thus, during stage A, a cake first formed and then became compressed. The solid-mass fraction was higher at the bottom of the cake than at the top, which is as expected for compressible cakes. During stage B, when water was filtered through the cake, the cake neither became compressed nor swelled. Finally, during stage C, the cake became compressed from the top until a constant solid-volume fraction was obtained throughout the cake. After roughly 40 min, the drainage process ended and the solid-mass fraction became constant and was measured to be 9.5% g/g. Hence, the final collapse resulted in a cake with a constant structural pressure throughout its thickness, indicating a cake with homogeneous water distribution. If the cake is consolidated after drainage, the best analytical models of the consolidation will, thus, be one in which it is assumed that the initial structural pressure is constant throughout the cake. Such a model has been derived in Shirato et al.¹⁸

The static compressibility of the dextran-MnO₂ cake was determined from drainage experiments in which the feed concentration was varied. As the solid-mass fraction was constant throughout the cake at the end of the experiment, it was possible to determine the cake compressibility by measuring the dry matter content at the end of the drainage experiment and compare it with the cake weight. Using data from the experiments shown in Table 1, it was found that the dry matter content increased with feed concentration. The sample volume was the same in all four experiments, and the increase in dry matter content was due to the higher weight of the formed cake. Equation 15 was used to calculate $f(\phi)$, setting $\phi_0 = 0.023$ as found in the previous presented sedimentation experiment. Figure 6 shows the final structural pressure throughout the cake as a function of $f(\phi)$. Equation 14 was fitted to the experimental data using linear regression; β was thereby estimated to be 0.33, and P_a esti-

mated to be 24 Pa. In the literature, β is regarded as a compressibility coefficient and a cake is termed highly compressible if $\beta > 0.25$.¹⁹ Furthermore, P_a was found to be lower than the pressure drop across the cake, i.e., 90–650 Pa. Thus, the estimated parameters indicate that the dextran-MnO₂ particles formed highly compressible cakes even at very low structural pressure. This has also been demonstrated in the case of biological sludge,²⁰ although the situation is very different from that observed for minerals. Hence, organic particles are also highly compressible at low pressure, and this must be incorporated into the drainage model as cake compression affects both drainage time and final dry matter content. Cake compression is a function of media resistance, feed concentration, and load.

Simulation of gravity drainage processes

The determined settling velocity, specific cake resistance and cake compressibility were then used as input parameters in simulating the entire drainage process. The simulations were performed numerically using Eqs. 2 and 3.

As the cake was compressible, the structural pressure in the cake was of particular interest because it influences the solid-mass fraction and, subsequently, the specific cake resistance. From the model, it is possible to simulate the structural pressure at the membrane-cake interface as $p_s = \eta R_{\text{mem}} v_f A^{-1}$. Figure 7 shows the simulated data. Different values for the media resistance have been used to demonstrate that the maximum structural pressure is strongly dependent on the media resistance. Consequently, the cake compression at the membrane is also expected to be strongly dependent on the media resistance. The initial pressure drop across the membrane is 650 Pa, and the calculated maximum structural pressure is shown in Table 2 at different membrane resistance values. For example, if R_{mem} is set to $8.1 \times 10^8 \text{ m}^{-1}$, the pressure at the bottom of the cake never exceeds the pressure throughout cake at the end of the experiment. The resistance of the media used was $9.7 \times 10^7 \text{ m}^{-1}$ and the

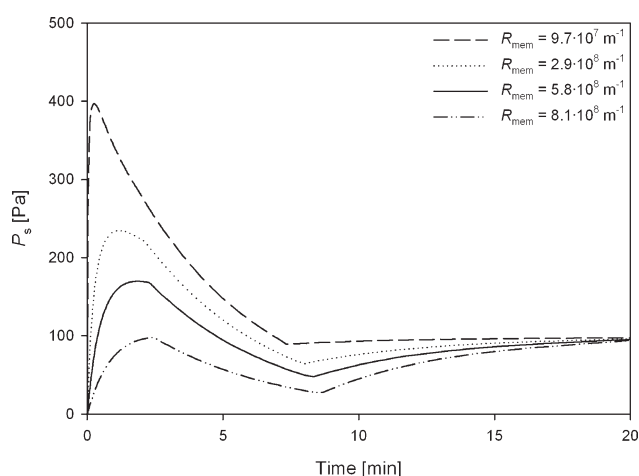


Figure 7. Simulated structural pressure at the sample-media interface for different media resistances.

Feed concentration has been set to 12 g/L. The specific cake resistance and compressibility data measured for cakes consisting of dextran-MnO₂ particles were been used in the simulation model.

Table 2. Simulated Maximum Structural Pressure at the Sample–Media Interface at Different Media Resistances*

Media resistance [m ⁻¹]	Max pressure [Pa]	Relative cake thickness
9.7×10^7	397	31%
2.9×10^8	234	66%
5.8×10^8	170	86%
8.1×10^8	98	100%

*The relative cake thickness at time of maximum pressure is also shown.

structural pressure at the bottom of the cake declined during drainage. Consequently, (1) the solid-mass fraction at the bottom should be higher than throughout the rest of the cake, or (2) cake compression should be reversible, so that the solid-mass fraction at the bottom of the cake decreases during the final part of the drainage process. This was not observed when the local solid-mass fraction was measured (Figure 5). According to the theory of highly compressible cakes, most of the pressure drop happens toward the very bottom of the cake.²¹ The resolution of the solid-mass fraction measurements was roughly 1 mm, so it was impossible to measure the solid-mass fraction just above the filter media. This could explain why it was impossible either to detect a solid-mass fraction gradient at the end of the process or to measure a decreasing solid-mass fraction near the cake bottom.

Figure 8 shows simulated values of the actual level of the suspension, h_t , together with the experimental data from Figure 3. The following input data were used in the model (solid line): $\alpha = 1.2 \times 10^9$ m/kg, $v_s = 1.6 \times 10^{-4}$ m/s, $h_{c,\infty} = 10.7$ mm, and $R_{\text{mem}} = 9.7 \times 10^7$ m⁻¹. The drainage rate is overestimated during the initial part of the experiment, so h_t decreases more rapidly than was observed during the experiment. This could be because the average specific cake resistance decreased during the drainage experiment due to cake compressibility and decreasing pressure across the cake. Initially, the structural pressure at the bottom of the cake was high, and the average specific cake resistance was high as well. After a while, the structural pressure declined

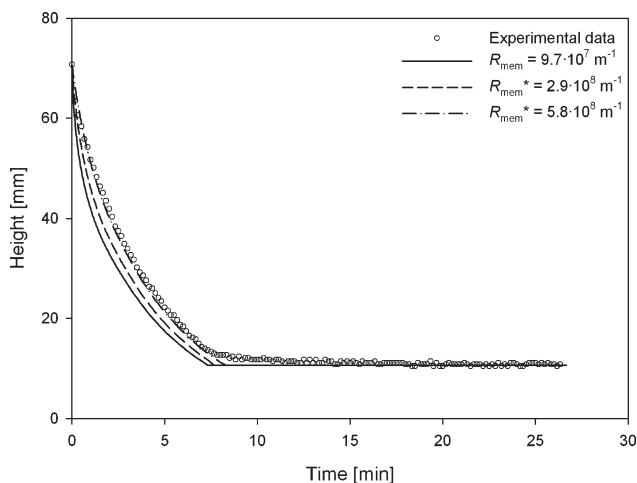


Figure 8. Experimental and simulated data for drainage of a suspension of 12 g/L dextran-MnO₂ particles (cf. Figure 3).

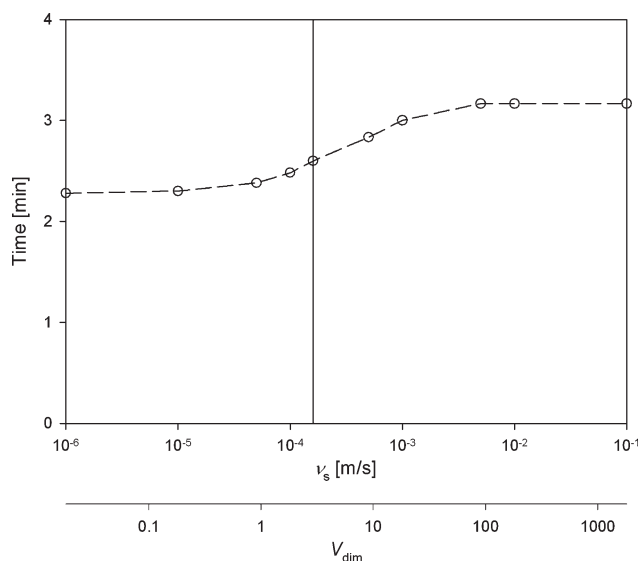


Figure 9. Impact of settling on the drainage process.

Nine simulations were carried out in which only the settling velocity was varied. The required time for draining 100 mL of the sample was found as a function of settling velocity. The vertical line indicates the actual measured settling velocity of dextran-MnO₂ particles.

and the newly formed cake structure was more loosely packed than it would have been if the pressure difference across the cake were constant during the experiment. This resulted in a decreasing average specific cake resistance. An apparent media resistance (R_{mem}^*) can be used to obtain a better fit (Figure 8). During the final cake collapse, a small deviation between the simulated and experimental data was observed, because the drag in the cake from the increasing capillary pressure was not incorporated into the model. To do so, it would be necessary to know the empirical parameters in Eq. 11, and model the local resistance and solid-mass fractions in the cake using a more complicated model. However, the error is small and the model is useful for evaluating how different input parameters influence drainage.

The model is used to study how the settling velocity influences the process. The largest difference between the simulated curves of h_t with and without settling is observed when approximately half the sample is drained. Thus, in Figure 9, the time required to drain 100 mL of the sample is plotted as a function of settling velocity. The required drainage time is short at a low-settling velocity, but increases when the settling velocity becomes comparable to the drainage rate. The time required to drain 100 mL increases by a maximum of 40% if the particles settle. As seen in Figure 9, settling becomes important for the drainage process if $v_s h_t$ is of the same order of magnitude or more than $v_d h_c$. Hence, the settling velocity v_s can be determined from a simple sedimentation experiment, and if $v_s h_t \ll v_d h_c$, settling does not influence the drainage model. In this situation, the settling velocity can be omitted from the simulation model, i.e., it can be assumed that cake height growth is proportional to filtrate volume. If the settling velocity is unknown, the maximum drainage rate can be calculated, assuming that the cake height grows proportionally with filtrate volume ($v_s = 0$), i.e., stage B will not appear. The minimum drainage rate can be calculated, assuming that the cake

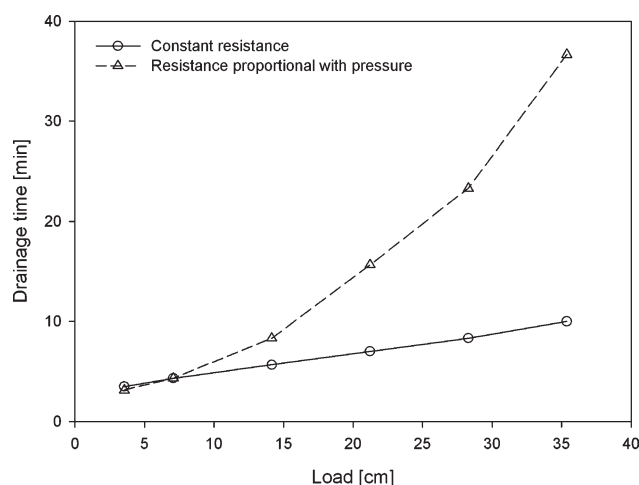


Figure 10. Impact of sample load on the drainage process.

Two series of six simulations were performed in which the load was varied. In series 1, it is assumed that the resistance was constant; in series 2, it is assumed that the resistance increases proportionally with pressure. The required time for draining 90% of the maximum possible drainage volume was then calculated as a function of load.

is fully buildup when the drainage process is started ($v_s \rightarrow \infty$), i.e., stage A will not appear.

The model simulation indicates that the required drainage time increases almost linearly with feed concentration; furthermore, the impact of the load has been studied as well. Figure 10 shows simulated data assuming a constant average specific cake resistance and a resistance that increases linearly with pressure. All input parameters are the same as used in Figure 8 where the load was 7.07 cm; at this load, the average specific cake resistance was set to 1.2×10^9 m/kg. It can be seen from Figure 10 that the required drainage time increases proportionally with load if the resistance is constant (i.e., in the case of noncompressible cakes); however, for highly compressible material, the required drainage time increases with load raised to the second power (highly compressible cakes). Thus, for highly compressible materials such as organic slurries, the load is very important for the drainage result. If the load is doubled, the drainage time increases by a factor of four assuming that the media resistance is negligible. At the end of the drainage process, a higher dry matter content of the cake will be observed if the load is doubled. Thus, there exists an optimum load, for example, on a filter press depending on drainage time (i.e., belt length and velocity) and media resistance. The feed concentration also influences the drainage rate and final dry matter content. The drainage rate increases proportionally with feed concentration, because a thicker cake is formed at a higher feed concentration. For the same reason, a higher dry matter content is obtained at the end of the drainage process if the feed concentration is increased. Now two alternative methods exist for increasing the final dry matter content of the cake: (1) increase the load, or (2) concentrate the feed. If possible, the best solution is to concentrate the feed before drainage, because the drainage time only increased by a factor of two when the feed concentration is doubled, not by a factor of four as observed when the load is doubled.

Conclusion

A mathematical model was developed to simulate drainage processes, and a new experimental method was used to determine needed input parameters: settling velocity, cake resistance and cake compressibility. Dextran-MnO₂ particle suspensions were drained, and it was found that the mathematical model fitted the experimental data well. Dextran-MnO₂ particles settled during drainage. However, settling only had a small impact on the drainage process. The drainage time was underestimated with less than 10% if settling was neglected during the simulation. The cake resistance was 1,000 times lower during drainage than during pressure filtrations. Thus, pressurized filtration resistances cannot be used for drainage simulations. Moreover, the formed cake was highly compressible also at the low pressure obtained during drainage. In the filtration step of the drainage process, a distinct increase of dry matter from top to bottom of the cake was observed. During the subsequent consolidation step, the cake compressed and a uniform dry matter profile was found. This is important. Due to cake compression, the dry matter content of a fully drained cake increases with both feed concentration and volumetric load. Furthermore, for highly compressible cake, the drainage time increased proportionally with *squared* volumetric load and not only linearly with load as for noncompressible materials. Thus, the effect of volumetric load on drainage time will be greatly underestimated if it is incorrectly assumed that the material is noncompressible.

Acknowledgments

This research was financed by the Danish Council for Technology and Innovation, grant number 274-07-0208. We thank Lisbeth Wybrandt and Ahmed Shamil Abdul Rahman for their technical assistance and Esbjerg Kommune for their help.

Notation

A = cross-sectional area of cylinder, m²
 c = solid concentration in feed, kg/m³
 h_0 = initial suspension level, m
 h_c = cake height, m
 h_s = distance between cake surface and sample-water interface, m
 h_t = actual suspension level, m
 h_w = height of clear water phase, m
 L = sample volume divided by cross-sectional area of cell, m
 M = sample mass, kg
 m = ratio of wet and dry cake mass, kg/kg
 P = applied pressure, Pa
 R_m = media resistance, m⁻¹
 S = ratio between dry mass of cake and total filtrate volume, kg/m³
 V_f = filtrate volume; equals $A(h_t - h_0)$, m³

Greek letters

α = specific filter cake resistance, m/kg
 ρ = filtrate density, kg/m³
 ρ_s = particle density, kg/m³
 $\Delta\rho$ = density difference between solid particle and liquid, kg/m³
 ϕ = cake solid-mass fraction, kg/kg
 ϕ = cake solid-volume fraction, m³/m³
 η = filtrate viscosity, Pa s
 v_d = drainage rate, m/s
 v_s = settling velocity, m/s
 μ = attenuation coefficient, m⁻¹
 ω = amount of disposed material per unit media area, kg/m²

Literature Cited

1. Cantrell KB, Ducey T, Ro KS, Hunt PG. Livestock waste-to-bioenergy generation opportunities. *Bioresour Technol.* 2008;99:7941–7953.
2. Rulkens W. Sewage sludge as a biomass resource for the production of energy: overview and assessment of the various options. *Energ Fuel.* 2008;22:9–15.
3. Severin BF, Grethlein HE. Laboratory simulation of belt press dewatering: application of the Darcy equation to gravity drainage. *Water Environ Res.* 1996;68:359–369.
4. Nielsen S. Sludge drying reed beds. *Water Sci Technol.* 2003;48:101–109.
5. Novak JT, Agerbaek ML, Sorensen BL, Hansen JA. Conditioning, filtering, and expressing waste activated sludge. *J Environ Eng ASCE.* 1999;125:816–824.
6. Wakeman RJ, Tarleton ES. *Filtration: Equipment Selection, Modelling and Process Simulation.* 1st ed. Oxford: Elsevier Science, Ltd; 1999.
7. Nenniger E, Storrow JA. Drainage of packed beds in gravitational and centrifugal-force fields. *AIChE J.* 1958;4:305–316.
8. Wakeman RJ, Vince A. Kinetics of gravity drainage from porous media. *Chem Eng Res Des.* 1986;64:94–103.
9. Severin BF, Nye JV, Kim BJ. Model and analysis of belt drainage thickening. *J Environ Eng ASCE.* 1999;125:807–815.
10. Richardson JF. Sedimentation and fluidisation: part 1. *T I Chem Eng.* 1954;32:S82–S99.
11. Hwang KJ, Lyu SY, Chen FF. The preparation and filtration characteristics of Dextran-MnO₂ gel particles. *Powder Technol.* 2006;161: 41–47.
12. Francis AW. Wall effect in falling ball method for viscosity. *Physics.* 1933;4:403–406.
13. Johansson C, Theliander H. Measuring concentration and pressure profiles in dead-end filtration. *Trans Filt Soc.* 2003;3:114–120.
14. Barr JD, White LR. Centrifugal drum filtration: II. A compression rheology model of cake draining. *AIChE J.* 2006;52:557–564.
15. Tiller FM, Leu WF. Basic data fitting in filtration. *J Chin Inst Chem Eng.* 1980;11:61–70.
16. Landman KA, White LR, Eberl M. Pressure filtration of flocculated suspensions. *AIChE J.* 1995;41:1687–1700.
17. Chen GW, Chang IL, Hung WT, Lee DJ. Regimes for zone settling of waste activated sludges. *Water Res.* 1996;30:1844–1850.
18. Shirato M, Murase T, Iwata M, Nakatsuka S. The Terzaghi-Voigt combined model for constant-pressure consolidation of filter cakes and homogeneous semisolid materials. *Chem Eng Sci.* 1986;41: 3213–3218.
19. Tiller FM, Kwon JH. Role of porosity in filtration XIII: behavior of highly compactible cakes. *AIChE J.* 1998;44:2159–2167.
20. Sørensen BL, Sørensen PB. Structure compression in cake filtration. *J Environ Eng ASCE.* 1997;123:345–353.
21. Sørensen PB, Hansen JA. Extreme solid compressibility in biological sludge dewatering. *Water Sci Technol.* 1993;28:133–143.

Manuscript received Oct. 7, 2009, and revision received Feb. 8, 2010.